X005

Near Surface Structures and Anisotropy from Cross-correlations of Ambient Seismic Noise at the Valhall Oil Field

A. Mordret* (IPGP), M. Landès (CEA), N.M. Shapiro (IPGP), S. Singh (IPGP), P. Roux (ISTerre) & O.I. Barkved (BP)

SUMMARY

We have used 6 hours of continuous vertical component geophone data from the Valhall Life of Field Seismic (LoFS) network to perform an Ambient Noise Surface Wave Tomography of the first hundreds meters of the Valhall field overburden to determine surface wave velocity. We were able to retrieve high-resolution features like paleo-channels that were previously highlighted by full waveform inversion of active source seismic data.

Furthermore, by computing the 2 690 040 cross-correlation functions between the full set of sensor pairs combinations, we were able to quantify the spatial distribution of azimuthal anisotropy over the whole network and link it to previous results from active seismic experiments.

Introduction

In active seismic dataset, the surface-waves energy represents more than two-thirds of the energy of the total wave-field (Park et al., 1999), it is then possible and easy to use the so-called ground-roll to perform near surface studies of the seafloor (Muyzert et al., 2002; Wills et al., 2008). However, such active seismic acquisitions, especially offshore, are very expensive and very time consuming. In this paper, we propose a method that overcomes these issues. It relies on the cross-correlation (CC) of seismic noise (e.g.,Gouedard et al., 2008) recorded by a large array: the Valhall Life of Field network. It has been shown theoretically that the Green's function (GF) of any inhomogeneous medium can be retrieved from the cross-correlation of sufficiently long recordings of a random wave field at different receiver locations (e.g., Weaver and Lobkis, 2001; Wapenaar, 2004; Gouedard et al., 2008). Most of studies using CCs focus on ocean microseism (0.03 - 1 Hz) which has its sources located at the interface of the oceans and the solid Earth (Longuet-Higgins, 1950; Kedar et al., 2008; Landès et al., 2010). As a consequence, the CCs are dominated by the fundamental mode of the surface-waves (Shapiro and Campillo, 2004). It is then possible to use those CCs in the same way as surface-waves from earthquakes or ground-roll from active seismic experiments to perform tomography (e.g., Shapiro et al., 2005).

Data processing

We used 6 hours of continuous recording of the vertical component from 2320 4C geophones of the Valhall LoFS network. The seismic noise pre-processing follows the procedure of Bensen et al., (2007): a single-station processing (separation of the traces in 1-minute long segments, temporal normalisation and spectral whitening) followed by the correlation of each segment for all possible pairs of stations and the stack of all correlations for each pair of stations. For this study, we used only the vertical component-to-vertical component correlation functions (CF).

Noise sources location

To assess the directivity of the waves that are reconstructed in the CF, we performed a beamforming analysis (e.g. Rost and Thomas, 2002) on the filtered CF of a 25-station sub-array with a distance of 4 km from the platform. This sub-array is made of three concentric circles with radii of 300 m, 600 m and 1200 m, centred at a station south-east of the platform, and the results of the beamforming are related to this position.

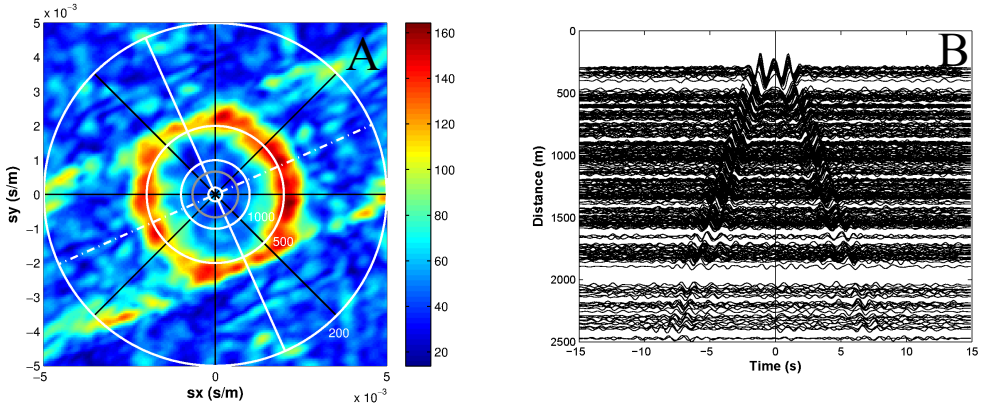

Figure 1 *A) Beamforming of the CF in the frequency range 0.4-2 Hz. B) 300 Correlation Functions filtered between 0.4 and 2 Hz sorted by increasing inter-station distance.*

The beamformer in the 0.4 - 2 Hz frequency range is shown on figure 1A; it is represented in the slowness plan: each circle stands for the velocity specified nearby, the grey circle is for the velocity 1500 m/s, the acoustic wave-speed in water. The white plain and dotted-dashed lines show respectively the principal azimuth of the Valhall network and its perpendicular. We can see that the retrieved waves are omnidirectional (the orange circular shape) and arrive with a velocity close to 400 m/s. When we filter the CF in this particular frequency band (figure 1B), we see that the CF are symmetrical and that these waves are dispersive Scholte's waves (Dellinger and Yu, 2009) and are suitable to perform a surface-wave tomography. The linear patterns perpendicular to the main direction of the LoFS array are aliasing artifacts due to the uneven distribution of sensors.

Ambient Noise Surface Wave Tomography

We used more than 184 000 CF extracted from station pairs separated between 1 km and 1.5 km. We computed the dispersion measurements using a Frequency-Time Analysis (FTAN, Levshin et al., 1989) over the negative, positive and symmetric (the average between the negative and the positive lags) parts of the CF at periods between 0.5 and 2 s. Theoretically, the dispersion curves of both three parts of the CF should be identical, thus, we used the difference between the negative and positive measurements to estimate the errors in the group-velocity measurements. We kept only the most accurate dispersion curves, i.e. when the difference between the negative and positive dispersion curves were smaller than 60 m/s, that had had for consequence to remove most of dispersion curves made from stations closer than 2 km from the exploitation platform at the centre of the array. The dispersion measurements of Scholte waves from 6 hours continuous data correlation were used to invert for group velocity maps on a 90 × 115 grid with 100 × 100 m cells size across the Valhall network using the surface-wave tomographic method of Barmin et al. (2001). Results at 0.8 s and 1.2 s are shown on figure 2.

Tomographic inversion results show sub-surface features like paleo-channels at different frequencies i.e. different depth that were previously highlighted by full waveform inversion of an active source seismic data (Sirgue et al., 2010). The high velocity ring around the platform at shallow depth might be related with the strong subsidence of the seafloor in the central area due to the depletion of the hydrocarbon reservoir at depth (Muyzert et al., 2002). Indeed, as shown with geomechanical modelling (Barkved et al., 2005; Hatchell et al., 2009), the subsidence creates a contractional strain at the centre of the bowl that can lead to an increase of the velocity.

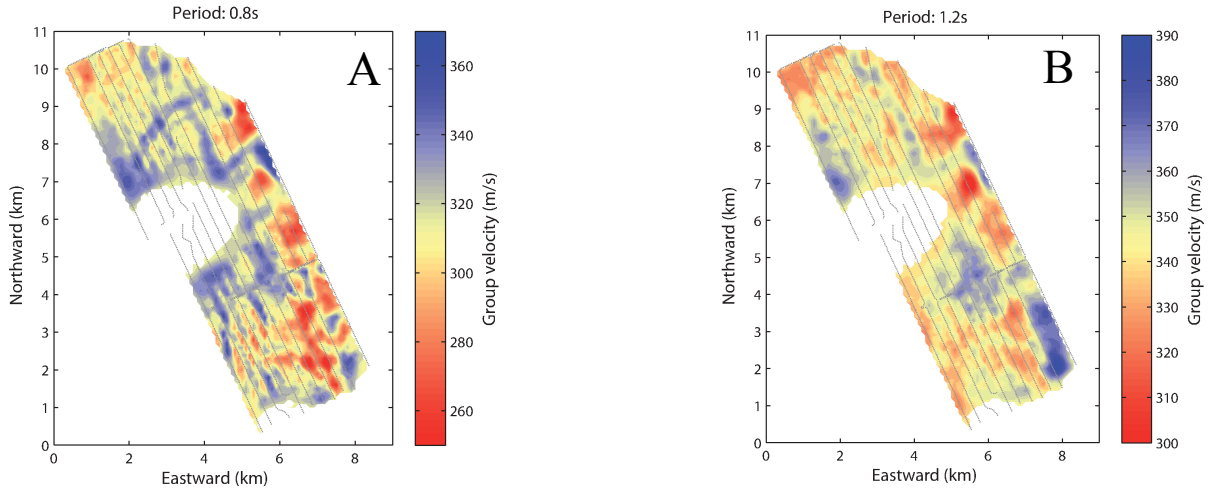

Figure 2 *A) Surface wave tomography map at 0.8 s. Clear paleo-channels are detectable as linear high velocity anomalies. B) Surface wave tomography map at 1.2 s. The large high velocity anomaly at the south-east is a part of a large meandering buried channel.*

Azimuthal anisotropy

Following Lin et al. (2009), we measured the phase velocity of the Scholte's waves between a central station and every station in a 500 m to 2 km ring around it for different periods. We computed the phase velocity variations as a function of the azimuth and we were able to retrieve the fast direction and the amplitude of the azimuthal anisotropy across the network.

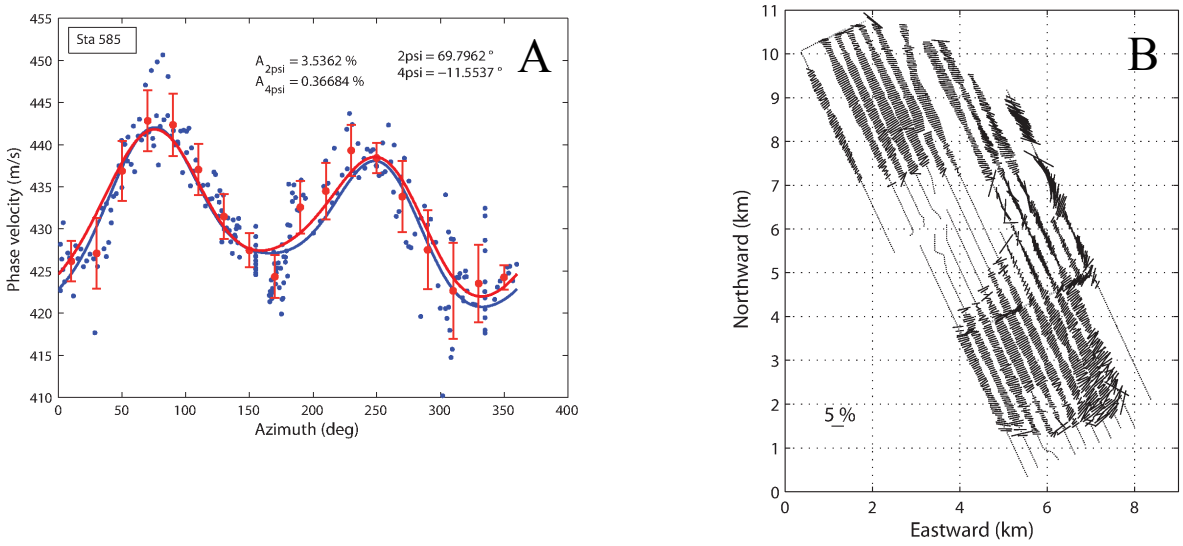

Figure 3 *A) Azimuthal distribution of the phase velocity at 0.8 s for the station 585. The blue dots are the phase velocity measurements. the red dots with error bars are the phase velocity averaged over 20°. The blue and red curves are the best fits for the 2ψ and 4ψ anisotropy variation for the raw and averaged velocity measurements respectively. B) Map of the 2ψ anisotropy at 0.8 s.*

We fitted the Smith and Dahlen (1973) azimuthal anisotropy formula to the data (figure 3A) for each station, based on signal-to-noise ratio criterion, to find the direction and amplitude of the fast direction anisotropy. The blue dots on figure 3A are the phase velocity measurements, the red dots with the error bars are the phase velocities averaged in 20° bins with their standard deviation and the blue and red curves are the least-square fitting to the raw and averaged data respectively. Figure 3B shows the map of the 2ψ anisotropy at 0.8 s. The clear circular pattern, already observed with shear-wave splitting measurements from active seismic data is the footprint of the local stress configuration created by the seafloor subsidence (Olofsson et al., 2003; Barkved et al., 2005; Zwartjes et al., 2008).

Conclusions

Our results demonstrated that only 6 hours of continuous "noise" signals recorded in a shallow water marine environment over the Valhall field contain significant amount of coherent energy that can be exploited with the cross-correlation approach. We could retrieve isotropic as well as anisotropic S-wave velocity information, which is a prelude to numerous applications in hydrocarbon exploration and exploitation fields.

Acknowledgements

We thank BP Norge AS and the Valhall partner, Hess Norge AS, granting access to the seismic data. The authors also acknowledge the use of resources provided by the European Grid Infrastructure. For more information, please consult the EGI-InSPIRE paper (http://go.egi.eu/pdnon).

References

- Barkved, O. I., T. Kristiansen, and E. Fjær, 2005, The 4D seismic response of a compacting reservoir - examples from the valhall field, norway: SEG Technical Program Expanded Abstracts, 24, 2508-2511.
- Barmin, M., Ritzwoller, M., & Levshin, A., 2001. A fast and reliable method for surface wave tomography, Pure and Applied Geophysics, 158(8), 1351–1375.
- Bensen, G., Ritzwoller, M., Barmin, M., Levshin, A., Lin, F., Moschetti, M., Shapiro, N., & Yang, Y., 2007. Processing seismic ambient noise data to obtain reliable broad-band surface wave dispersion measurements, Geophysical Journal International, 169(3), 1239–1260.
- Dellinger, J. and Yu, J., 2009. Low-frequency virtual point-source interferometry using conventional sensors, 71st EAGE Conference, Extended Abstract, X047.
- Gouedard, P., L. Stehly, F. Brenguier, M. Campillo, Y. Colin de Verdiere, E. Larose, L. Margerin, P. Roux, F. Sanchez-Sesma, N. Shapiro, and R.Weaver, 2008. Cross-correlation of random fields: mathematical approach and applications, Geophysical prospecting, 56(3), 375-393.
- Hatchell, P.J., Wills, P.B. & Didraga, C., 2009. Production Induced Effects on Near-surface Wave Velocities at Valhall, 71st EAGE Conference, Paper T016.
- Kedar, S., M. Longuet-Higgins, F.Webb, N. Graham, R. Clayton, and C. Jones, 2008. The origin of deep ocean microseisms in the north atlantic ocean, Proceedings of the Royal Society A: Mathematical, Physical and Engineering Science, 464(2091), 777.
- Landès, M., F. Hubans, N. Shapiro, A. Paul, and M. Campillo, 2010. Origin of deep ocean microseisms by using teleseismic body waves, Journal of Geophysical Research, 115, B05,302.
- Levshin, A., Yanovskaya, T., Lander, A., Bukchin, B., Barmin, M., Ratnikova, L., & Its, E., 1989. Seismic surface waves in a laterally inhomogeneous Earth, Kluwer, Dordrecht.
- Lin, F., M. Ritzwoller, and R. Snieder, 2009. Eikonal tomography: surface wave tomography by phase front tracking across a regional broad-band seismic array, Geophysical Journal International, 177(3), 1091-1110.
- Longuet-Higgins, M., 1950. A theory of the origin of microseisms, Philosophical Transactions of the Royal Society of London. Series A, Mathematical and Physical Sciences, 243(857), 1-35.
- Muyzert, E., J. H. Kommedal, K. Iranpour, and B. Olofsson, 2002. Near-surface s-velocities, statics, and anisotropy estimated from scholte waves: 64th Annual EAGE Conference, Paper F28.
- Olofsson B., Probert T., Kommedal J. H. & Barkved O. I., 2003, Azimuthal anisotropy from the Valhall 4C 3D survey, The Leading Edge, 22, 1228
- Park, C., R. Miller, and J. Xia, 1999. Multichannel analysis of surface waves, Geophysics, 64, 800.
- Rost, S. & Thomas, C., 2002. Array seismology: methods and applications, Review of Geophysics, 40(3), 1008.
- Shapiro, N. and M. Campillo, 2004. Emergence of broadband Rayleigh waves from correlations of the ambient seismic noise, Geophysical Research Letters, 31(7), 1615-1619.
- Shapiro, N., Campillo, M., Stehly, L., & Ritzwoller, M., 2005. High-resolution surface-wave tomography from ambient seismic noise, Science, 307(5715), 1615.
- Sirgue, L., Barkved, O., Dellinger, J., Etgen, J., Albertin, U., & Kommedal, J., 2010. Full waveform inversion: the next leap forward in imaging at Valhall, First Break, 28, 65-70.
- Smith, M., and F. Dahlen, 1973. The azimuthal dependence of Love and Rayleigh wave propagation in a slightly anisotropic medium, Journal of Geophysical Research, 78(17), 3321{3333}.
- Wapenaar, K., 2004. Retrieving the elastodynamic Green's function of an arbitrary inhomogeneous medium by cross correlation, Physical Review Letters, 93(25), 254,301.
- Weaver, R., and O. Lobkis, 2001. Ultrasonics without a source: Thermal Fluctuation correlations at MHz frequencies, Physical Review Letters, 87(13), 134,301.
- Wills, PB., PJ. Hatchell and SJ. Bourne, 2008. Time-lapse Measurements of Shallow Horizontal Wave Velocity over a Compacting Field. 70th EAGE Conference and Exhibition, Extended Abstract, G039.
- Zwartjes, P., P. Wills, J. De Maag, and P. Hatchell, 2008. Shallow and Deep Time-lapse Effects on Valhall LoFS Converted Wave Data, in 70th EAGE Conference and Exhibition, Extended Abstract, G040.